Topological Quantum Criticality in the Quasiperiodic Cluster Ising Chain

Sheng Yang,[1] Hai-Qing Lin,[1,*] and Xue-Jia Yu[2,†]
[1]Institute for Advanced Study in Physics and School of Physics, Zhejiang University, Hangzhou 310058, China
[2]Eastern Institute of Technology, Ningbo 315200, China

(Received 3 February 2026; revised 19 July 2026; accepted 26 October 2026; published 19 November 2026)

Topological classifications of quantum critical systems have recently attracted growing interest, as they go beyond the traditional paradigms of condensed matter and statistical physics. However, such classifications remain largely unexplored in aperiodic environments, particularly under quasiperiodic modulations. In this Letter, we uncover a family of topological quasiperiodic fixed points with critical scalings intermediate between the clean and infinite-randomness limits. By exactly solving the quasiperiodic cluster Ising chain, we demonstrate that all phase boundaries separating quasiperiodically modulated phases are governed by topological Ising-like fixed points unique to strongly modulated quasiperiodic systems. Although their local bulk critical properties match those of conventional quasiperiodic Ising critical points reported before, these fixed points host robust topological edge degeneracies and exhibit a distinct symmetry-enriched realization of the quasiperiodic Ising criticality, as further supported by complementary lattice simulations.

DOI: 10.1103/l8m8-vk2h

Introduction—Discovering universality classes of phase transitions that go beyond the conventional Landau-Ginzburg-Wilson symmetry-breaking paradigm constitutes a central theme in modern statistical and condensed-matter physics. For decades, the classification of universality classes was long believed to be uniquely determined by a set of critical exponents, forming the standard framework for investigating phase transitions both theoretically and experimentally [1–3]. This belief has been challenged by recent advances in the discovery of topological physics in quantum critical systems [4–8]. In particular, symmetry-protected topological edge modes—previously thought to exist only in gapped systems—have been shown to coexist with a gapless bulk at criticality, resulting in topologically distinct realizations of the same universality class even when they share the same local bulk critical exponents, now referred to as topologically nontrivial or symmetry-enriched quantum critical points (QCPs) [7–28], and more generally to gapless symmetry-protected topological (SPT) states [5,7,29–48]. The corresponding edge state can also be systematically constructed within the framework of conformal field theory (CFT) [49–57]. This conceptual extension not only generalizes the notion of topology to gapless quantum critical systems but also reveals fundamentally new phenomena beyond gapped topological phases, including nontrivial conformal boundary conditions [8,58–62], algebraically localized edge modes [7,39], universal bulk-boundary correspondence [20,25,32,48], anomalous dynamical scaling behaviors [27,63], and intrinsically gapless topological states [29,34,38,40].

A natural and pressing question is how such topological quantum criticality manifests in realistic settings, where imperfections and inhomogeneities are unavoidable and may profoundly modify the universality classes of phase transitions [64–68]. A particularly intriguing form of imperfection in many modern experimental platforms—including superconducting qubit arrays [69,70], moiré materials [71,72], and cold atoms in bichromatic optical lattices [73–75]—is intrinsic inhomogeneity arising from quasiperiodic (QP) modulations of the couplings. These modulations can be regarded as a form of correlated randomness and are, therefore, expected to realize universality classes absent in both clean and randomly disordered systems. Nevertheless, over the past decades, studies of phase transitions in QP systems have focused primarily on localization-delocalization phenomena [76–93], particularly the pioneering works of Kohmoto and collaborators, which revealed new localization transitions, scaling behavior, and critical (multifractal) spectra [94–97]. By contrast, *ground-state* quantum phase transitions in such systems—despite recent progress [98–116]—are far less explored. Previous works have argued that clean critical points are perturbatively more stable against QP than random perturbations, based on the general stability criterion proposed by Luck [68]. However, a more fundamental and intriguing

*Contact author: hqlin@zju.edu.cn
†Contact author: xuejiayu@eitech.edu.cn

Published by the American Physical Society under the terms of the Creative Commons Attribution 4.0 International license. Further distribution of this work must maintain attribution to the author(s) and the published article's title, journal citation, and DOI.

open question concerns how strong QP modulations interplay with topology and whether they can give rise to QCPs that are genuinely distinct from those in conventional homogeneous systems.

In this Letter, we fill this gap by uncovering a family of topological quasiperiodic fixed points unique to QP modulated systems. By analytically establishing the ground-state phase diagram of the QP cluster Ising spin chain, we first show that strong QP modulations induce an unconventional topological phase with area-law entanglement despite a vanishing bulk energy gap. More importantly, we unambiguously demonstrate that, although all phase boundaries separating quasiperiodically modulated phases lack CFT descriptions, they can still be enriched by certain global symmetries, giving rise to topological critical points with robust topological edge degeneracies and critical scalings intermediate between the clean and infinite-randomness limits. Consequently, the QP cluster Ising transition identified here is topologically distinct from the previously recognized QP-Ising transition in Ref. [101], as they cannot be smoothly connected without encountering a multicritical point or explicitly breaking the protecting symmetries.

Model—We consider a spin-1/2 cluster Ising chain [6–8] with QP modulations,

$$H_{\mathrm{CI}}^{\mathrm{QP}} = -\sum_i J_i \sigma_i^x \sigma_{i+1}^x - \sum_i g_i \sigma_i^x \sigma_{i+1}^z \sigma_{i+2}^x, \tag{1}$$

which preserves a $\mathbb{Z}_2$ spin-flip symmetry generated by $P = \prod_i \sigma_i^z$ and a time-reversal symmetry $\mathbb{Z}_2^T$ generated by $T = K$ the complex conjugation. Together they form the protecting symmetry $G = \mathbb{Z}_2 \times \mathbb{Z}_2^T$. In particular, the QP modulated couplings are chosen as [our conclusions apply to generic continuous strong QP modulations for which the couplings vanish at certain lattice sites [109], as illustrated in Fig. 1(b)]

$$J_i = \bar{J} + h_J \cos[Q(i+1/2) + \phi_1], \tag{2}$$

$$g_i = \bar{g} + h_g \cos[Qi + \phi_1 + \phi_2]. \tag{3}$$

Here, $\sigma_i^{x,y,z}$ denote Pauli matrices at site i, and J_i (g_i) are the QP modulated Ising (cluster) couplings with modulation strengths h_J (h_g). The modulation is quasiperiodic when the wavelength $2\pi/Q$ is an irrational multiple of the lattice constant $a = 1$. In this Letter, we set $Q/(2\pi) = \tau_{\mathrm{G}}$, with $\tau_{\mathrm{G}} = (\sqrt{5}+1)/2$ the Golden ratio. In numerical simulations with periodic boundary conditions (PBCs), we employ rational approximants $Q/(2\pi) = p_i/q_i = F_{i+2}/F_{i+1}$, where F_i are Fibonacci numbers. This approximation can be viewed as a periodic spin chain with q_i local degrees of freedom per unit cell. At criticality, the low-energy theory is expected to be described by a multicomponent or orbifold CFT, $(\text{Ising CFT})^{q_i}/\mathbb{Z}_{q_i}$ [117] for sufficiently large system sizes commensurate with q_i, and by a defect CFT when the system size is incommensurate [118–124]. However, since our Letter focuses on QP quantum criticality, the scaling analysis is restricted to length scales $r < q_i$, where such emergent CFT or defect-CFT descriptions do not arise. Accordingly, the system size is set to $N = 2q_i$, which ensures that the modulation is commensurate with the lattice periodicity. The associated period q_i, thus, provides a sequence of finite length scales for scaling analysis. Hereafter, we denote q_i simply as q for brevity. For open boundary conditions (OBCs), we fix $Q/(2\pi)$ directly to τ_{G}. Our results are not restricted to this choice and apply to a broad class of irrational wave vectors [see Sec. III of Supplemental Material [125] for details]. The phases ϕ_1 and ϕ_2 shift the modulations relative to the lattice; most of the calculations presented below involve averaging over different samples of $\phi_{1/2}$ to obtain reliable critical scaling while reducing the system-size requirements; for wandering, however, fixed phases are used, as all configurations are effectively represented within a single large system [65,131,132].

Ground-state phase diagram—In this Letter, we focus on the *ground-state* properties of QP systems, rather than on localization or dynamical phenomena that are more commonly studied in the literature. The QP cluster Ising model defined in Eq. (1) is exactly solvable via a Jordan-Wigner transformation, enabling us to analytically establish its ground-state phase diagram [101,109] (also see Supplemental Material, Sec. I [125]), shown in Fig. 1(c).

In the weak-modulation regime ($\bar{J} = \bar{g} > h_J, h_g$), the QP perturbation is irrelevant, and the symmetry-enriched phase boundaries (see the End Matter for a brief review) between the ferromagnetic (FM) and the $\mathbb{Z}_2 \times \mathbb{Z}_2^T$ cluster SPT phase are preserved. In contrast, the strong-modulation regime ($\bar{J} = \bar{g} < h_J, h_g$) hosts two distinct gapless phases separated by three phase boundaries. One is a QP-FM phase that has been studied previously [100,109], while the other is an unconventional SPT phase that exhibits area-law entanglement scaling despite a vanishing bulk energy gap—a feature unique to QP systems—which we refer to as the QP-SPT phase (see End Matter for details). The central question addressed in this Letter is whether symmetry-enriched quantum criticality persists under strong QP modulation, and whether such topological quantum criticality is intrinsic to QP settings.

Quasiperiodic Ising universality class—We now turn to the phase transitions in the presence of strong QP modulation. In the main text, we focus on a representative strongly modulated critical point at $\bar{J} = \bar{g} = 1/2$ and $h_J = h_g = 1$ [the red star in Fig. 1(c)], which separates the QP-SPT and QP-FM phases. For comparison, we also analyze the weakly modulated Ising transition at $\bar{J} = \bar{g} = 1/2$ and $h_J = h_g = 1/3$ [the black square in Fig. 1(c)], where the QP modulation is irrelevant [68,101] and belongs to clean symmetry-enriched universality. Throughout this Letter, we focus on mean-averaged physical observables (see End

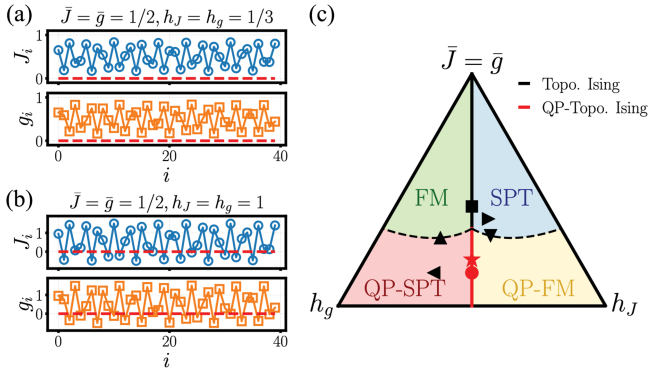


FIG. 1. (a),(b) Spatial profiles of couplings J_i and g_i for two representative points marked in (c) (black square and red star). Parameters: fixed $\phi_1 = 1/10$ and $\phi_2 = 1$. (c) Ground-state phase diagram of the QP cluster Ising model containing FM, QP-FM, SPT, and QP-SPT phases. The vertical black and red lines represent the topological Ising and QP-topological Ising critical lines, respectively. Symbols indicate points analyzed in later figures.

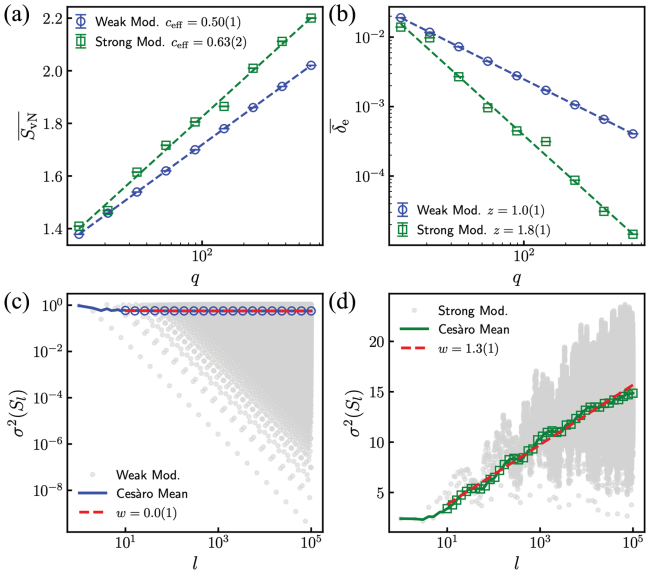


FIG. 2. (a) Logarithmic-law behavior of the half-chain entanglement entropy $\overline{S_{\text{vN}}} = (c_{\text{eff}}/3)\ln q + \text{const.}$ (b) Energy gap $\overline{\delta_e}$ versus q for strongly and weakly modulated QCP. The dashed lines represent fits to the scaling form $\overline{\delta_e}(q) \sim 1/q^z$. (c),(d) Variance of the wandering $\sigma^2(S_l)$ as a function of l for weakly and strongly modulated QCPs, respectively. The blue and green lines are Cesàro means, and the red dashed lines are fits of $\sigma^2(S_l) \propto w \log(l)$; the markers represent the data used in fits. Parameters: $\bar{J} = \bar{g} = 1/2, h_J = h_g = 1$ [the red star in Fig. 1(c)] for strongly modulated QCP and $\bar{J} = \bar{g} = 1/2, h_J = h_g = 1/3$ [the black square in Fig. 1(c)] for the weakly modulated QCP. The parameter q ranges from 13 to 610 under PBC for (a) and (b). In (c) and (d), we have fixed $\phi_1 = 1/10$ and $\phi_2 = 1$.

Matter), which exhibit scaling behaviors analogous to those of homogeneous systems but with modified exponent values. We first demonstrate that the QP critical points identified here are intermediate between those of clean and infinite-randomness fixed points.

To examine whether QP modulation is sufficient to drive the critical point of the cluster Ising model into the infinite-randomness regime, we investigate the entanglement properties at both critical points through finite-size scaling of the averaged half-chain entanglement entropy $\overline{S_{\text{vN}}}$, as shown in Fig. 2(a). At both transitions, $\overline{S_{\text{vN}}}$ grows logarithmically with system size but with distinct prefactors. This indicates that, despite the absence of conformal invariance at the strongly modulated critical point, the averaged entanglement entropy nevertheless follows the standard $(1+1)$-dimensional CFT scaling form known from clean systems [133], albeit with an effective central charge $c_{\text{eff}} = 0.63(2)$, which differs from both the clean ($c = 1/2$) and the infinite randomness Ising QCP ($c_{\text{eff}} = \frac{1}{2}\ln 2$ [9]). The salient features of this QP fixed point are further corroborated by the finite-size scaling of the bulk energy gap [Fig. 2(b)], which exhibits algebraic scaling $\overline{\delta_e} \sim q^{-z}$ at both the weakly (blue curve) and strongly modulated (green curve) transition points, with dynamical critical exponents $z \approx 1.0$ and $z = 1.8(1)$, respectively. Note that the latter is also consistent with the value reported for the strongly modulated QP transverse-field Ising chain [101,109], which also constitutes the initial evidence that the bulk critical behavior of the QP cluster Ising critical point we found matches that of the QP trivial Ising one as detailed further below. This behavior indicates that, although strong QP modulation in our context breaks conformal invariance at criticality, it is insufficient to drive the transition to an infinite-randomness fixed point (IRFP) that is characterized by exponentially fast gap closing ($z = \infty$); it also rules out the recently proposed infinite-quasiperiodic transition scenario [104,105] (see End Matter for more discussion). Moreover, infinite-randomness physics is typically accompanied by qualitatively distinct scaling of the typical and arithmetic averaged spin correlation functions—exponential decay for the former and algebraic decay for the latter (see Supplemental Material, Sec. II [125] and the following section). By contrast, at the QP-Ising transition, no such distinction is observed: the typical and arithmetic averaged spin correlations exhibit the same qualitative power-law scaling, providing further evidence against infinite-randomness criticality.

Another way to substantiate the intermediate universality unique to QP systems is through an analysis of the wandering [68], which captures the leading effect of QP modulation on the critical cluster Ising chain. Specifically, the wandering $S_l(j) = \sum_{i=j}^{j+l-1} \ln(|J_i/g_i|)$ quantifies fluctuations of the reduced coupling J_i/g_i summed over a segment of length l. More importantly, the scaling behavior of the wandering variance $\sigma^2(S_l) = [S_l(j)^2] - [S_l(j)]^2$, where $[\cdot]$ means the average over the site position j, serves as a diagnostic of different types of disordered criticality [109,134]. In $(1+1)$ dimensions, $\sigma^2(S_l)$ saturates to a

constant at a clean critical point, while it grows linearly with l at an uncorrelated disordered critical point. By contrast, at a QP critical point, $\sigma^2(S_l)$ exhibits logarithmic scaling, $\sigma^2(S_l) \sim w \ln l$, with a nonvanishing coefficient w, known as the logarithmic wandering coefficient [101]. In practice, we characterize the scaling behavior of $\sigma^2(S_l)$ at both critical points using the Cesàro mean, $[\sigma^2(S_l)]_{\text{Cesàro}} = (1/l)\sum_{l'=1}^{l} \sigma^2(S_{l'})$. As shown in Figs. 2(c) and 2(d), $[\sigma^2(S_l)]_{\text{Cesàro}}$ saturates to a constant at the weakly modulated critical point [blue curve in Fig. 2(c)], whereas it exhibits logarithmic growth only at the strongly modulated critical point, with a coefficient $w \simeq 1.3(1)$ [green curve in Fig. 2(d)], consistent with analytical results for the QP transverse-field Ising chain [109]. We, therefore, conclusively demonstrate that the strongly modulated critical point is controlled by a QP-Ising fixed point intermediate between the clean and infinite-randomness limits.

Topological features at quasiperiodic transition—Recent advances [4,6,8] have demonstrated that two QCPs can be further distinguished by their topological properties even when they share the same local bulk critical exponents and are, therefore, controlled by distinct fixed points, as they cannot be smoothly connected without either crossing an additional phase transition or breaking the protecting symmetries. It is, therefore, necessary to determine whether the QP Ising fixed point found here is topologically distinct from the critical point of the QP transverse-field Ising chain reported in the literature [101,109].

A key hallmark of topologically nontrivial QCPs is that their local bulk properties are indistinguishable from those of the trivial critical point, while nontrivial topological features manifest on nonlocal string operators, entanglement-spectrum degeneracies, and boundary properties. To demonstrate this in our setting, we compare various properties at the transition points of the QP cluster-Ising chain and the QP transverse-field Ising chain [101,109]. Specifically, we first examine the averaged bulk-bulk spin correlation function $\overline{C_{\text{FM}}(r)}$ under PBCs at criticality, as shown in Fig. 3(a). In both cases, the rescaled correlator $q^{2\Delta_\sigma^{\text{bulk}}}\overline{C_{\text{FM}}(r)}$ collapses onto a single curve when plotted as a function of the fractional separation r/q, with a common bulk scaling dimension $\Delta_\sigma^{\text{bulk}} = 0.18(1)$ (see Supplemental Material, Sec. II [125] for the results of the bulk-bulk energy-energy correlation). By contrast, the boundary critical behaviors of the two QP-Ising fixed points is clearly distinguished by the averaged boundary-bulk spin correlation function [see Fig. 3(b)], which both exhibits power-law decay of the form $r^{-(\Delta_\sigma^{\text{bulk}}+\Delta_\sigma^{\text{bdy}})}$ but with significantly different boundary scaling dimensions: $\Delta_\sigma^{\text{bdy}} = 0.59(2)$ for the QP-Ising and $\Delta_\sigma^{\text{bdy}} = 1.6(1)$ for the QP cluster Ising fixed point (see Supplemental Material, Sec. II [125] for the results of the boundary-bulk energy-energy correlation). Taken together, while the QP cluster-Ising fixed point

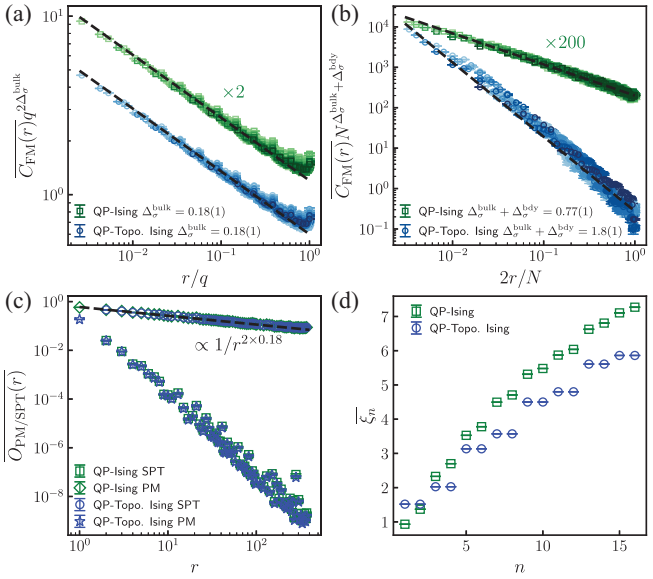


FIG. 3. Data collapse of (a) bulk-bulk and (b) boundary-bulk connected correlation functions $\overline{C_{\text{FM}}(r)}$ for QP-topological Ising and QP-Ising transitions. The dashed lines are $\propto 1/(r/q)^{2\Delta_\sigma^{\text{bulk}}}$ or $\propto 1/(2r/N)^{\Delta_\sigma^{\text{bulk}}+\Delta_\sigma^{\text{bdy}}}$ for comparison with the data collapse. To achieve a better visualization, we have multiplied an additional global factor for the correlations of QP Ising as indicated by "×2" and "×200." (c) The power-law behaviors of SPT and PM string orders; the corresponding scaling dimensions are extracted via data collapse shown in Supplemental Material, Sec. II [125]. (d) The bulk many-body entanglement spectrum $\overline{\xi_n}$. Parameters: $\overline{J} = \bar{g} = 1/2, h_J = h_g = 1$. The parameter q ranges from 13 to 377 under PBC for (a) and N ranges from 100 to 600 under OBC for (b). In (c) and (d), we have chosen $q = 377$ and 610, respectively, under PBC.

identified here shares indistinguishable local bulk critical properties with the QP-Ising critical point proposed in Refs. [101,109], it exhibits fundamentally different boundary behaviors, which can be attributed to nontrivial topological edge degeneracy, as discussed below. It is noted that the concrete values of the exponents extracted here also support that the QP-Ising transition is different from the clean Ising or IRFP (see Table I for a detailed comparison).

To further elucidate the topological distinction between the two QP critical points, we note that, although conformal symmetry is absent under strong QP modulation, both QP Ising fixed points—analogously to the Ising CFT—have nonlocal μ operators that carry distinct time-reversal symmetry charges, $T\mu T = \pm\mu$, providing a definite bulk topological invariant. Here, μ denotes the leading $\mathbb{Z}_2$ symmetry-flux operator, identified by the slowest decay of its two-point function. On the lattice, these operators take the same form of nonlocal string operators as in the clean Ising model, but with modified scaling dimensions—their averaged two-point functions are $\overline{O_{\text{PM}}(r)}$ for the QP-Ising transition and $\overline{O_{\text{SPT}}(r)}$ for the QP cluster Ising transition—indeed, the nearby QP modulated symmetric phases are

TABLE I. Comparison of bulk $\Delta_\sigma^{\text{bulk}}$ and boundary $\Delta_\sigma^{\text{bdy}}$ scaling dimensions of the spin operator across three cases: Ising, IRFP, and QP Ising. $\mathbb{Z}_2^T$ denotes the time-reversal symmetry and $\tau_G = (1+\sqrt{5})/2$.

	Trivial		Enriched by $\mathbb{Z}_2^T$	
System type	$\Delta_\sigma^{\text{bulk}}$	$\Delta_\sigma^{\text{bdy}}$	$\Delta_\sigma^{\text{bulk}}$	$\Delta_\sigma^{\text{bdy}}$
Clean Ising [8]	1/8	1/2	1/8	2
IRFP [9]	$1-\tau_G/2$	1/2	$1-\tau_G/2$	0
QP Ising	0.18(1)	0.59(2)	0.18(1)	1.6(1)

still probed by the same order parameters. This topological invariant cannot change under continuous $\mathbb{Z}_2 \times \mathbb{Z}_2^T$-preserving deformations that retain QP-Ising criticality. Opposite time-reversal charges, therefore, distinguish different symmetry-enriched realizations of QP-Ising criticality, leading to topologically distinct QP-Ising fixed points without CFT descriptions.

These predictions are tested numerically. As shown in Fig. 3(c), we compute the averaged string operators $\overline{O_{\text{PM}}(r)}$ and $\overline{O_{\text{SPT}}(r)}$ at both transitions. At the QP cluster Ising critical point, $\overline{O_{\text{SPT}}(r)}$ exhibits a slower algebraic decay than $\overline{O_{\text{PM}}(r)}$, whereas the situation is reversed at the QP-Ising critical point. These results imply that the two QP-Ising critical points are topologically distinct, exhibiting qualitatively different condensation behaviors of the nonlocal μ operators. At the QP transverse-field Ising critical point, the condensation of the $\mathbb{Z}_2^T$-neutral μ operator preserves the $\mathbb{Z}_2$ symmetry near the boundary. In contrast, at the QP cluster Ising critical point, condensation of the $\mathbb{Z}_2^T$-charged μ operator is prohibited, stabilizing a boundary condition with spontaneously broken $\mathbb{Z}_2$ symmetry and an associated twofold topological degeneracy. As a result, the two transitions exhibit distinct boundary critical behaviors, in agreement with the numerical results shown in Fig. 3(b). Complementarily, we examine the averaged bulk entanglement spectrum $\overline{\xi_n}$ at both transition points [Fig. 3(d)], observing a robust twofold topological degeneracy at the QP cluster Ising QCP (blue dots) (see also Supplemental Material, Sec. II [125] for its robustness against symmetry-preserving perturbations), whereas no such degeneracy is present at the conventional QP-Ising QCP (green squares). Taken together, these results uncover that time-reversal symmetry can enrich QP critical points even in the absence of conformal symmetry, yielding a symmetry-enriched realization of QP-Ising criticality that is topologically distinct from the conventional one, as summarized in Table I.

Discussion and concluding remarks—In Supplemental Material, Secs. II and IV [125], we further examine additional representative points along the QP-SPT to QP-FM phase boundary, which exhibit scaling exponents closely matching those discussed in the main text, suggesting that the entire phase boundary realizes the same topologically nontrivial QP-Ising criticality. Moreover, we show that quasiperiodic and topological characteristics persist qualitatively—albeit with different scaling exponents—at selected points along the other two phase boundaries that separate the QP-SPT and FM phases, as well as the QP-FM and cluster SPT phases. Therefore, we believe that phase boundaries between SPT and symmetry-breaking phases, when at least one phase is strongly quasiperiodically modulated, are controlled by a continuous line of topological QP fixed points. Numerical exploration of such QP fixed points faces substantial challenges, including the strong-disorder renormalization-group methods suitable for IRFPs, as well as tensor-network and quantum Monte Carlo simulations that require demanding computational resources, highlighting the advantage of the exact solution used here.

In summary, we reveal a topological Ising-like criticality in strongly QP-modulated systems. By exactly solving the QP cluster Ising chain, we establish the ground-state phase diagram and uncover an unconventional QP-SPT phase in which gapped SPT order coexists with vanishing bulk energy gap—a phenomenon distinctive of strong quasiperiodicity. More importantly, we unambiguously demonstrate that global symmetry can further enrich strongly QP-modulated phase boundaries that lack a CFT description, giving rise to topological QP critical points with critical scalings intermediate between the clean and infinite-randomness limits, as supported by complementary lattice simulations. The measured local bulk critical scaling agrees with that of the conventional QP-Ising transition within numerical accuracy, while the leading symmetry-flux operator carries a different time-reversal charge. The two transitions, thus, exhibit distinct symmetry-enriched realizations of the QP-Ising universality under the $\mathbb{Z}_2 \times \mathbb{Z}_2^T$ protecting symmetry. This distinction is preserved under symmetry-preserving deformations that retain the QP-Ising criticality.

In the near future, it would be particularly interesting to explore the dynamical and localization properties of symmetry-enriched QP fixed points, as topology and QP modulation are each known to have distinct and profound effects on these phenomena. It is also worthwhile to develop efficient algorithms for studying QP criticality in the presence of interactions. From an experimental perspective, the cluster Ising chain has recently been realized in ultracold-atom [135,136] and superconducting qubit quantum platforms [21], where QP couplings can also be conveniently engineered and controlled within the same settings.

Acknowledgments—We thank Romain Vasseur, Yuxuan Guo, Wen-Yuan Liu, Xiang-Ping Jiang, and Kaiyuan Cao for helpful discussions. X.-J. Y. was supported by the

National Natural Science Foundation of China (Grant No. 12405034) and a start-up grant from Eastern Institute of Technology, Ningbo. This work is also supported by MOST 2022YFA1402701. The work of S. Y. is supported by China Postdoctoral Science Foundation (Certificate No. 2024M752760).

Data availability—The data are not publicly available. The data are available from the authors upon reasonable request.

[1] L. D. Landau and E. M. Lifshitz, *Statistical Physics: Volume 5* (Elsevier, Oxford, 2013), Vol. 5.
[2] S. Sachdev, Quantum phase transitions, Phys. World **12**, 33 (1999).
[3] S. L. Sondhi, S. M. Girvin, J. P. Carini, and D. Shahar, Continuous quantum phase transitions, Rev. Mod. Phys. **69**, 315 (1997).
[4] X.-J. Yu, L. Xu, and H.-Q. Lin, Topological physics in quantum critical systems, Phys. Rep. **1160**, 1 (2026).
[5] T. Scaffidi, D. E. Parker, and R. Vasseur, Gapless symmetry-protected topological order, Phys. Rev. X **7**, 041048 (2017).
[6] R. Verresen, N. G. Jones, and F. Pollmann, Topology and edge modes in quantum critical chains, Phys. Rev. Lett. **120**, 057001 (2018).
[7] R. Verresen, R. Thorngren, N. G. Jones, and F. Pollmann, Gapless topological phases and symmetry-enriched quantum criticality, Phys. Rev. X **11**, 041059 (2021).
[8] X.-J. Yu, R.-Z. Huang, H.-H. Song, L. Xu, C. Ding, and L. Zhang, Conformal boundary conditions of symmetry-enriched quantum critical spin chains, Phys. Rev. Lett. **129**, 210601 (2022).
[9] C. M. Duque, H.-Y. Hu, Y.-Z. You, V. Khemani, R. Verresen, and R. Vasseur, Topological and symmetry-enriched random quantum critical points, Phys. Rev. B **103**, L100207 (2021).
[10] R. Verresen, Topology and edge states survive quantum criticality between topological insulators, arXiv:2003.05453.
[11] W. Ye, M. Guo, Y.-C. He, C. Wang, and L. Zou, Topological characterization of Lieb-Schultz-Mattis constraints and applications to symmetry-enriched quantum criticality, SciPost Phys. **13**, 066 (2022).
[12] S. Mondal, A. Agarwala, T. Mishra, and A. Prakash, Symmetry-enriched criticality in a coupled spin ladder, Phys. Rev. B **108**, 245135 (2023).
[13] X.-J. Yu and W.-L. Li, Fidelity susceptibility at the Lifshitz transition between the noninteracting topologically distinct quantum critical points, Phys. Rev. B **110**, 045119 (2024).
[14] W. Choi, M. Knap, and F. Pollmann, Finite-temperature entanglement negativity of fermionic symmetry-protected topological phases and quantum critical points in one dimension, Phys. Rev. B **109**, 115132 (2024).
[15] W.-H. Zhong, W.-L. Li, Y.-C. Chen, and X.-J. Yu, Topological edge modes and phase transitions in a critical fermionic chain with long-range interactions, Phys. Rev. A **110**, 022212 (2024).
[16] S. Prembabu, R. Thorngren, and R. Verresen, Boundary-deconfined quantum criticality at transitions between symmetry-protected topological chains, Phys. Rev. B **109**, L201112 (2024).
[17] L. Li, R.-Z. Huang, and W. Cao, Noninvertible symmetry-enriched quantum critical point, Phys. Rev. B **112**, L081113 (2025).
[18] L. Zhou, J. Gong, and X.-J. Yu, Topological edge states at Floquet quantum criticality, Commun. Phys. **8**, 214 (2025).
[19] G. Cardoso, H.-C. Yeh, L. Korneev, A. G. Abanov, and A. Mitra, Gapless Floquet topology, Phys. Rev. B **111**, 125162 (2025).
[20] W.-H. Zhong, H.-Q. Lin, and X.-J. Yu, Quantum entanglement of fermionic symmetry-enriched quantum critical points in one dimension, Phys. Rev. B **112**, 075129 (2025).
[21] Z. Tan *et al.*, Exploring nontrivial topology at quantum criticality on a superconducting processor, Commun. Phys. **9**, 136 (2026).
[22] K.-H. Chou, X.-J. Yu, and P.-Y. Chang, $\mathcal{PT}$ symmetry-enriched non-unitary criticality, arXiv:2509.09587.
[23] A. Rey, Ö. M. Aksoy, D. P. Arovas, C. Chamon, and C. Mudry, Incommensurate gapless ferromagnetism connecting competing symmetry-enriched deconfined quantum phase transitions, Phys. Rev. B **112**, L161110 (2025).
[24] B. Moy, Generalized symmetry enriched criticality in $(3+1)$d, SciPost Phys. **19**, 145 (2025).
[25] Y. Guo, S. Yang, and X.-J. Yu, Generalized Li-Haldane correspondence in critical free-fermion systems, Phys. Rev. Res. **8**, 023203 (2026).
[26] S. Prembabu, S.-H. Shao, and R. Verresen, Non-invertible interfaces between symmetry-enriched critical phases, arXiv:2512.23706.
[27] M. Deng, C. Sun, F. Li, and X.-J. Yu, Anomalous dynamical scaling at topological quantum criticality, Phys. Rev. Lett. **137**, 096605 (2026).
[28] H. Jia, J. Hu, R.-Y. Zhang, Y. Xiao, D. Wang, M. Wang, S. Ma, X. Ouyang, Y. Zhu, and C. T. Chan, Unconventional topological edge states in one-dimensional non-hermitian gapless systems stemming from nonisolated hypersurface singularities, Phys. Rev. Lett. **134**, 206603 (2025).
[29] R. Thorngren, A. Vishwanath, and R. Verresen, Intrinsically gapless topological phases, Phys. Rev. B **104**, 075132 (2021).
[30] Y. Hidaka, S. C. Furuya, A. Ueda, and Y. Tada, Gapless symmetry-protected topological phase of quantum antiferromagnets on anisotropic triangular strip, Phys. Rev. B **106**, 144436 (2022).
[31] R. Wen and A. C. Potter, Bulk-boundary correspondence for intrinsically gapless symmetry-protected topological phases from group cohomology, Phys. Rev. B **107**, 245127 (2023).
[32] X.-J. Yu, S. Yang, H.-Q. Lin, and S.-K. Jian, Universal entanglement spectrum in one-dimensional gapless symmetry protected topological states, Phys. Rev. Lett. **133**, 026601 (2024).
[33] L. Su and M. Zeng, Gapless symmetry-protected topological phases and generalized deconfined critical points from gauging a finite subgroup, Phys. Rev. B **109**, 245108 (2024).

[34] H.-L. Zhang, H.-Z. Li, S. Yang, and X.-J. Yu, Quantum phase transition and critical behavior between the gapless topological phases, Phys. Rev. A **109**, 062226 (2024).

[35] L. Li, M. Oshikawa, and Y. Zheng, Decorated defect construction of gapless-SPT states, SciPost Phys. **17**, 013 (2024).

[36] R. Wen, W. Ye, and A. C. Potter, Topological holography for fermions, arXiv:2404.19004.

[37] S.-J. Huang, Fermionic quantum criticality through the lens of topological holography, arXiv:2405.09611.

[38] L. Li, M. Oshikawa, and Y. Zheng, Intrinsically/purely gapless-SPT from non-invertible duality transformations, SciPost Phys. **18**, 153 (2025).

[39] S. Yang, H.-Q. Lin, and X.-J. Yu, Gapless topological behaviors in a long-range quantum spin chain, Commun. Phys. **8**, 27 (2025).

[40] S. Yang, F. Xu, D.-C. Lu, Y.-Z. You, H.-Q. Lin, and X.-J. Yu, Deconfined criticality as intrinsically gapless topological state in one dimension, Phys. Rev. B **113**, L201105 (2026).

[41] R. Wen, String condensation and topological holography for $2+1$D gapless SPT, arXiv:2408.05801.

[42] X.-J. Yu, S. Yang, S. Liu, H.-Q. Lin, and S.-K. Jian, Gapless symmetry-protected topological states in measurement-only circuits, Phys. Rev. B **113**, 134302 (2026).

[43] R. Wen and A. C. Potter, Classification of $1+1$D gapless symmetry protected phases via topological holography, Phys. Rev. B **111**, 115161 (2025).

[44] R. Flores-Calderón, E. J. König, and A. M. Cook, Topological quantum criticality from multiplicative topological phases, Phys. Rev. Lett. **134**, 116602 (2025).

[45] S.-J. Huang and M. Cheng, Topological holography, quantum criticality, and boundary states, SciPost Phys. **18**, 213 (2025).

[46] R. Wen, Topological holography for $2+1$-D gapped and gapless phases with generalized symmetries, arXiv:2503.13685.

[47] S. Prembabu and R. Verresen, Multicriticality between purely gapless SPT phases with unitary symmetry, arXiv:2509.20431.

[48] A. Banerjee and M. Zeng, Entanglement spectrum of gapless topological phases: A case study with topological superconductors, Phys. Rev. B **114**, 055104 (2026).

[49] K. Graham and G. M. Watts, Defect lines and boundary flows, J. High Energy Phys. 04 (2004) 019.

[50] J. Fröhlich, J. Fuchs, I. Runkel, and C. Schweigert, Kramers-wannier duality from conformal defects, Phys. Rev. Lett. **93**, 070601 (2004).

[51] S. C. Furuya and M. Oshikawa, Symmetry protection of critical phases and a global anomaly in $1+1$ dimensions, Phys. Rev. Lett. **118**, 021601 (2017).

[52] P. Lecheminant, Massless renormalization group flow in $SU(N)_k$ perturbed conformal field theory, Nucl. Phys. **B901**, 510 (2015).

[53] Y. Fukusumi and S. Iino, Open spin chain realization of a topological defect in a one-dimensional Ising model: Boundary and bulk symmetry, Phys. Rev. B **104**, 125418 (2021).

[54] Y.-H. Wu, Y. Zhang, H.-H. Tu, and M. Cheng, Impurity screening by defects in $(1+1)d$ quantum critical systems, Phys. Rev. Lett. **136**, 036502 (2026).

[55] M. Okada and Y. Tachikawa, Noninvertible symmetries act locally by quantum operations, Phys. Rev. Lett. **133**, 191602 (2024).

[56] I. Runkel and G. M. T. Watts, Fermionic CFTs and classifying algebras, J. High Energy Phys. 06 (2020) 025.

[57] P. B. Smith, Boundary states and anomalous symmetries of fermionic minimal models, arXiv:2102.02203.

[58] S. Fredenhagen, Organizing boundary RG flows, Nucl. Phys. **B660**, 436 (2003).

[59] G. M. Watts, On the renormalisation group for the boundary truncated conformal space approach, Nucl. Phys. **B859**, 177 (2012).

[60] I. Affleck and A. W. W. Ludwig, Universal noninteger ground-state degeneracy in critical quantum systems, Phys. Rev. Lett. **67**, 161 (1991).

[61] D. Friedan and A. Konechny, Boundary entropy of one-dimensional quantum systems at low temperature, Phys. Rev. Lett. **93**, 030402 (2004).

[62] D. E. Parker, T. Scaffidi, and R. Vasseur, Topological Luttinger liquids from decorated domain walls, Phys. Rev. B **97**, 165114 (2018).

[63] D. E. Parker, R. Vasseur, and T. Scaffidi, Topologically protected long edge coherence times in symmetry-broken phases, Phys. Rev. Lett. **122**, 240605 (2019).

[64] T. Vojta, Disorder in quantum many-body systems, Annu. Rev. Condens. Matter Phys. **10**, 233 (2019).

[65] D. S. Fisher, Random transverse field Ising spin chains, Phys. Rev. Lett. **69**, 534 (1992).

[66] D. S. Fisher, Critical behavior of random transverse-field Ising spin chains, Phys. Rev. B **51**, 6411 (1995).

[67] O. Motrunich, S.-C. Mau, D. A. Huse, and D. S. Fisher, Infinite-randomness quantum Ising critical fixed points, Phys. Rev. B **61**, 1160 (2000).

[68] J. M. Luck, Critical behavior of the aperiodic quantum Ising chain in a transverse magnetic field, J. Stat. Phys. **72**, 417 (1993).

[69] Y.-H. Shi *et al.*, Quantum simulation of topological zero modes on a 41-qubit superconducting processor, Phys. Rev. Lett. **131**, 080401 (2023).

[70] W. Huang *et al.*, Observation of exact quantum critical states, Nat. Phys. **22**, 1209 (2026).

[71] A. Uri, S. C. de la Barrera, M. T. Randeria, D. Rodan-Legrain, T. Devakul, P. J. D. Crowley, N. Paul, K. Watanabe, T. Taniguchi, R. Lifshitz, L. Fu, R. C. Ashoori, and P. Jarillo-Herrero, Superconductivity and strong interactions in a tunable moiré quasicrystal, Nature (London) **620**, 762 (2023).

[72] X. Lai, G. Li, A. M. Coe, J. H. Pixley, K. Watanabe, T. Taniguchi, and E. Y. Andrei, Moiréperiodic and quasiperiodic crystals in heterostructures of twisted bilayer graphene on hexagonal boron nitride, Nat. Mater. **24**, 1019 (2025).

[73] P. Bordia, H. Lüschen, S. Scherg, S. Gopalakrishnan, M. Knap, U. Schneider, and I. Bloch, Probing slow relaxation and many-body localization in two-dimensional quasiperiodic systems, Phys. Rev. X **7**, 041047 (2017).

[74] B. Deissler, M. Zaccanti, G. Roati, C. D'Errico, M. Fattori, M. Modugno, G. Modugno, and M. Inguscio, Delocalization of a disordered bosonic system by repulsive interactions, Nat. Phys. **6**, 354 (2010).

[75] H. P. Lüschen, P. Bordia, S. S. Hodgman, M. Schreiber, S. Sarkar, A. J. Daley, M. H. Fischer, E. Altman, I. Bloch, and U. Schneider, Signatures of many-body localization in a controlled open quantum system, Phys. Rev. X **7**, 011034 (2017).
[76] S. Aubry and G. André, Analyticity breaking and Anderson localization in incommensurate lattices, Ann. Isr. Phys. Soc. **3**, 133 (1980).
[77] P. G. Harper, Single band motion of conduction electrons in a uniform magnetic field, Proc. Phys. Soc. London Sect. A **68**, 874 (1955).
[78] S. Das Sarma, S. He, and X. C. Xie, Mobility edge in a model one-dimensional potential, Phys. Rev. Lett. **61**, 2144 (1988).
[79] J. Ringot, P. Szriftgiser, J. C. Garreau, and D. Delande, Experimental evidence of dynamical localization and delocalization in a quasiperiodic driven system, Phys. Rev. Lett. **85**, 2741 (2000).
[80] F. Evers and A. D. Mirlin, Anderson transitions, Rev. Mod. Phys. **80**, 1355 (2008).
[81] J. Biddle, B. Wang, D. J. Priour, and S. Das Sarma, Localization in one-dimensional incommensurate lattices beyond the Aubry-André model, Phys. Rev. A **80**, 021603 (2009).
[82] J. Biddle and S. Das Sarma, Predicted mobility edges in one-dimensional incommensurate optical lattices: An exactly solvable model of Anderson localization, Phys. Rev. Lett. **104**, 070601 (2010).
[83] S. Iyer, V. Oganesyan, G. Refael, and D. A. Huse, Many-body localization in a quasiperiodic system, Phys. Rev. B **87**, 134202 (2013).
[84] S. Ganeshan, J. H. Pixley, and S. Das Sarma, Nearest neighbor tight binding models with an exact mobility edge in one dimension, Phys. Rev. Lett. **114**, 146601 (2015).
[85] V. Khemani, D. N. Sheng, and D. A. Huse, Two universality classes for the many-body localization transition, Phys. Rev. Lett. **119**, 075702 (2017).
[86] H. Yao, A. Khoudli, L. Bresque, and L. Sanchez-Palencia, Critical behavior and fractality in shallow one-dimensional quasiperiodic potentials, Phys. Rev. Lett. **123**, 070405 (2019).
[87] S. Longhi, Topological phase transition in non-hermitian quasicrystals, Phys. Rev. Lett. **122**, 237601 (2019).
[88] E. V. H. Doggen and A. D. Mirlin, Many-body delocalization dynamics in long Aubry-André quasiperiodic chains, Phys. Rev. B **100**, 104203 (2019).
[89] N. Macé, N. Laflorencie, and F. Alet, Many-body localization in a quasiperiodic Fibonacci chain, SciPost Phys. **6**, 050 (2019).
[90] Y. Wang, X. Xia, L. Zhang, H. Yao, S. Chen, J. You, Q. Zhou, and X.-J. Liu, One-dimensional quasiperiodic mosaic lattice with exact mobility edges, Phys. Rev. Lett. **125**, 196604 (2020).
[91] T. Lv, T.-C. Yi, L. Li, G. Sun, and W.-L. You, Quantum criticality and universality in the p-wave-paired Aubry-André-Harper model, Phys. Rev. A **105**, 013315 (2022).
[92] M. Gonçalves, B. Amorim, E. V. Castro, and P. Ribeiro, Critical phase dualities in 1D exactly solvable quasiperiodic models, Phys. Rev. Lett. **131**, 186303 (2023).
[93] C. Yang, W. Yang, Y. Wang, and Y. Wang, Exploring multifractal critical phases in two-dimensional quasiperiodic systems, Phys. Rev. A **110**, 042205 (2024).
[94] M. Kohmoto, L. P. Kadanoff, and C. Tang, Localization problem in one dimension: Mapping and escape, Phys. Rev. Lett. **50**, 1870 (1983).
[95] M. Kohmoto, B. Sutherland, and C. Tang, Critical wave functions and a cantor-set spectrum of a one-dimensional quasicrystal model, Phys. Rev. B **35**, 1020 (1987).
[96] M. Kohmoto, Metal-insulator transition and scaling for incommensurate systems, Phys. Rev. Lett. **51**, 1198 (1983).
[97] H. Hiramoto and M. Kohmoto, New localization in a quasiperiodic system, Phys. Rev. Lett. **62**, 2714 (1989).
[98] F. J. Oliveira Filho, M. S. Faria, and A. P. Vieira, Strong-disorder renormalization group study of aperiodic quantum Ising chains, J. Stat. Mech. (2012) P03007.
[99] K. Deguchi, S. Matsukawa, N. K. Sato, T. Hattori, K. Ishida, H. Takakura, and T. Ishimasa, Quantum critical state in a magnetic quasicrystal, Nat. Mater. **11**, 1013 (2012).
[100] A. Chandran and C. R. Laumann, Localization and symmetry breaking in the quantum quasiperiodic Ising glass, Phys. Rev. X **7**, 031061 (2017).
[101] P. J. D. Crowley, A. Chandran, and C. R. Laumann, Quasiperiodic quantum Ising transitions in 1D, Phys. Rev. Lett. **120**, 175702 (2018).
[102] U. Divakaran, Sudden quenches in a quasiperiodic Ising model, Phys. Rev. E **98**, 032110 (2018).
[103] P. J. D. Crowley, C. R. Laumann, and S. Gopalakrishnan, Quantum criticality in Ising chains with random hyperuniform couplings, Phys. Rev. B **100**, 134206 (2019).
[104] U. Agrawal, S. Gopalakrishnan, and R. Vasseur, Universality and quantum criticality in quasiperiodic spin chains, Nat. Commun. **11**, 2225 (2020).
[105] U. Agrawal, S. Gopalakrishnan, and R. Vasseur, Quantum criticality in the 2D quasiperiodic potts model, Phys. Rev. Lett. **125**, 265702 (2020).
[106] T. Cookmeyer, J. Motruk, and J. E. Moore, Critical properties of the ground-state localization-delocalization transition in the many-particle Aubry-André model, Phys. Rev. B **101**, 174203 (2020).
[107] B. S. Revathy and U. Divakaran, Adiabatic dynamics of quasiperiodic transverse Ising model, J. Stat. Mech. (2020) 023108.
[108] M. Khosravian and J. L. Lado, Quasiperiodic criticality and spin-triplet superconductivity in superconductor-antiferromagnet moiré patterns, Phys. Rev. Res. **3**, 013262 (2021).
[109] P. J. D. Crowley, C. R. Laumann, and A. Chandran, Critical behaviour of the quasi-periodic quantum Ising chain, J. Stat. Mech. (2022) 083102.
[110] L. Yeo and P. J. D. Crowley, Universal nonpower law scaling from a chaotic renormalization group in the Harper-Hofstadter model, Phys. Rev. Lett. **137**, 096303 (2026).
[111] G. Shkolnik, A. Zabalo, R. Vasseur, D. A. Huse, J. H. Pixley, and S. Gazit, Measurement induced criticality in quasiperiodic modulated random hybrid circuits, Phys. Rev. B **108**, 184204 (2023).

[112] J. F. Karcher, R. Vasseur, and S. Gopalakrishnan, Extended critical phase in quasiperiodic quantum Hall systems, Phys. Rev. B **109**, 064208 (2024).

[113] M. Gonçalves, J. H. Pixley, B. Amorim, E. V. Castro, and P. Ribeiro, Short-range interactions are irrelevant at the quasiperiodicity-driven luttinger liquid to Anderson glass transition, Phys. Rev. B **109**, 014211 (2024).

[114] M. Gonçalves, Entanglement entropy scaling in critical phases of one-dimensional quasiperiodic systems, Phys. Rev. B **109**, 104202 (2024).

[115] T. J. Vongkovit, H. Singh, R. Vasseur, and S. Gopalakrishnan, Effective Luttinger parameter and Kane-Fisher effect in quasiperiodic systems, Phys. Rev. B **110**, L020201 (2024).

[116] C. Zhang, Y.-K. Yu, S.-H. Shi, and Z.-X. Li, Magnetic order and novel quantum criticality in the strongly interacting quasicrystals, arXiv:2512.13546.

[117] P. Francesco, P. Mathieu, and D. Sénéchal, *Conformal Field Theory* (Springer Science & Business Media, New York, 2012).

[118] F. C. Alcaraz, M. N. Barber, and M. T. Batchelor, Conformal invariance, the XXZ chain and the operator content of two-dimensional critical systems, Ann. Phys. (N.Y.) **182**, 280 (1988).

[119] V. Petkova and J.-B. Zuber, Generalised twisted partition functions, Phys. Lett. B **504**, 157 (2001).

[120] H. Watanabe, M. Cheng, and Y. Fuji, Ground state degeneracy on torus in a family of $\mathbb{Z}_N$ toric code, J. Math. Phys. (N.Y.) **64**, 051901 (2023).

[121] Y. Hu and H. Watanabe, Spontaneous symmetry breaking without ground state degeneracy in generalized n-state clock model, Phys. Rev. B **107**, 195139 (2023).

[122] A. Roy and H. Saleur, Entanglement entropy in the Ising model with topological defects, Phys. Rev. Lett. **128**, 090603 (2022).

[123] H. Schlömer, C. Tan, S. Haas, and H. Saleur, Parity effects and universal terms of $\mathcal{O}(1)$ in the entanglement near a boundary, SciPost Phys. **13**, 110 (2022).

[124] C. Northe and P. Rossi, Entanglement through topological defects: Reconciling theory with numerics, arXiv:2512.07974.

[125] See Supplemental Material at http://link.aps.org/supplemental/10.1103/l8m8-vk2h, which includes Refs. [7–9, 109,126–130], for I. Details of the analytical calculations of the quasi-periodic cluster-Ising chain; II. Additional numerical results of the transition between the QP-FM and QP-SPT phases; III. Numerical results for the Silver ratio; and IV. Numerical results for the remaining two phase boundaries.

[126] G. B. Mbeng, A. Russomanno, and G. E. Santoro, The quantum Ising chain for beginners, SciPost Phys. Lect. Notes, 82 (2024).

[127] M.-C. Chung and I. Peschel, Density-matrix spectra of solvable fermionic systems, Phys. Rev. B **64**, 064412 (2001).

[128] S.-A. Cheong and C. L. Henley, Many-body density matrices for free fermions, Phys. Rev. B **69**, 075111 (2004).

[129] I. Peschel and V. Eisler, Reduced density matrices and entanglement entropy in free lattice models, J. Phys. A **42**, 504003 (2009).

[130] N. Chepiga and N. Laflorencie, Resilient infinite randomness criticality for a disordered chain of interacting Majorana fermions, Phys. Rev. Lett. **132**, 056502 (2024).

[131] E. Miranda and V. Dobrosavljevic, Disorder-driven non-Fermi liquid behaviour of correlated electrons, Rep. Prog. Phys. **68**, 2337 (2005).

[132] T. Vojta, Rare region effects at classical, quantum and nonequilibrium phase transitions, J. Phys. A **39**, R143 (2006).

[133] P. Calabrese and J. Cardy, Entanglement entropy and quantum field theory, J. Stat. Mech. (2004) P06002.

[134] S. Torquato, Hyperuniformity and its generalizations, Phys. Rev. E **94**, 022122 (2016).

[135] F. Petiziol, M. Sameti, S. Carretta, S. Wimberger, and F. Mintert, Quantum simulation of three-body interactions in weakly driven quantum systems, Phys. Rev. Lett. **126**, 250504 (2021).

[136] S. de Léséleuc, V. Lienhard, P. Scholl, D. Barredo, S. Weber, N. Lang, H. P. Büchler, T. Lahaye, and A. Browaeys, Observation of a symmetry-protected topological phase of interacting bosons with Rydberg atoms, Science **365**, 775 (2019).

[137] H. Li and F. D. M. Haldane, Entanglement spectrum as a generalization of entanglement entropy: Identification of topological order in non-Abelian fractional quantum hall effect states, Phys. Rev. Lett. **101**, 010504 (2008).

[138] M. B. Hastings, An area law for one-dimensional quantum systems, J. Stat. Mech. (2007) P08024.

[139] J. Eisert, M. Cramer, and M. B. Plenio, Colloquium: Area laws for the entanglement entropy, Rev. Mod. Phys. **82**, 277(C) (2010).

[140] D. Boyanovsky and J. L. Cardy, Critical behavior of m-component magnets with correlated impurities, Phys. Rev. B **26**, 154 (1982).

[141] Y. B. Kim and X.-G. Wen, Large-N renormalization-group study of the commensurate dirty-boson problem, Phys. Rev. B **49**, 4043 (1994).

[142] J. Ye, S. Sachdev, and N. Read, Solvable spin glass of quantum rotors, Phys. Rev. Lett. **70**, 4011 (1993).

[143] D. Bernard, (Perturbed) conformal field theory applied to 2D disordered systems an introduction, arXiv:hep-th/9509137.

[144] Z. Maassarani and D. Serban, Non-unitary conformal field theory and logarithmic operators for disordered systems, Nucl. Phys. **B489**, 603 (1997).

[145] V. S. Dotsenko, X. S. Nguyen, and R. Santachiara, Models WD_n in the presence of disorder and the coupled models, Nucl. Phys. **B613**, 445 (2001).

[146] B. M. McCoy and T. T. Wu, Theory of a two-dimensional Ising model with random impurities. I. Thermodynamics, Phys. Rev. **176**, 631 (1968).

[147] B. M. McCOY and T. T. WU, Theory of a two-dimensional Ising model with random impurities. II. Spin correlation functions, Phys. Rev. **188**, 982 (1969).

[148] R. B. Griffiths, Nonanalytic behavior above the critical point in a random Ising ferromagnet, Phys. Rev. Lett. **23**, 17 (1969).

End Matter

Brief review of the symmetry-enriched Ising CFT—We briefly illustrate the physics of symmetry-enriched criticality [7] by considering the quantum phase transitions in the transverse-field Ising and cluster Ising chain, both of which possess a global spin-flip $\mathbb{Z}_2$ symmetry and a spinless time-reversal symmetry $\mathbb{Z}_2^T$. These transitions are described by the $(1+1)$D Ising CFT, featuring a unique local scaling operator σ and a *unique* nonlocal scaling operator μ, both with scaling dimension $\Delta_{\sigma/\mu} = 1/8$ [117]. At the lattice level, the local scaling operator σ serves as the FM order parameter, while the nonlocal scaling operator μ corresponds to the Kramers-Wannier dual string order parameter of the symmetric phase—namely, the PM string operator in the transverse-field Ising model [see Eq. (B2)] and the SPT string operator in the cluster Ising model [see Eq. (B3)]. The nonlocal string operators can be interpreted as symmetry fluxes [7] that carry distinct time-reversal symmetry charge, $T\mu T = \pm\mu$, and exhibit the *slowest* algebraic decay at both critical points, distinguishing two symmetry-enriched realizations of the same Ising CFT with distinct conformal boundary conditions [8,62]. Importantly, these two realizations are topologically distinct and cannot be smoothly connected without encountering a multicritical point or explicitly breaking the protecting symmetries.

This picture also applies to the quasiperiodic setup studied in this Letter. It is noted that, physically, the distinct boundary criticalities exhibited by the trivial and topological QP-Ising critical points are not mere boundary artifacts of a single bulk fixed point. Instead, they are intrinsically rooted in the nontrivial bulk topological features of the quantum critical points, analogous to the bulk-boundary correspondence in gapped topological phases. Consequently, although their measured local bulk critical exponents agree within numerical accuracy, these critical points exhibit distinct symmetry-enriched realizations of the QP-Ising criticality. To further substantiate this distinction, we map out the global phase diagram of a generalized quasiperiodic Ising Hamiltonian that interpolates between these two regimes and identify a multicritical point separating the two critical lines within the symmetry-preserving parameter space (see Sec. II of Supplemental Material [125] for numerical results).

Physical observables—To characterize the rich phase diagram and critical behaviors of the model, we calculate various connected correlation functions and string order parameters. To detect the ferromagnetic (FM) order, we compute the spin-spin correlation,

$$C_{\mathrm{FM}}(r) = \langle \sigma_i^x \sigma_{i+r}^x \rangle - \langle \sigma_i^x \rangle \langle \sigma_{i+r}^x \rangle. \tag{B1}$$

The trivial paramagnetic (PM) phase is characterized by the nonlocal PM string operator,

$$O_{\mathrm{PM}}(r) = \left\langle \prod_{k=i}^{i+r-1} \sigma_k^z \right\rangle. \tag{B2}$$

To identify the symmetry-protected topological (SPT) cluster phase, we employ the SPT string order parameter,

$$O_{\mathrm{SPT}}(r) = \left\langle \sigma_i^x \sigma_{i+1}^y \left(\prod_{k=i+2}^{i+r-1} \sigma_k^z \right) \sigma_{i+r}^y \sigma_{i+r+1}^x \right\rangle. \tag{B3}$$

To complementarily characterize the nontrivial boundary critical behavior of the model, we consider the energy-energy correlation,

$$C_{\mathrm{EN}}(r) = \langle \epsilon_i \epsilon_{i+r} \rangle - \langle \epsilon_i \rangle \langle \epsilon_{i+r} \rangle, \tag{B4}$$

where the local energy operator is defined as $\epsilon_i \equiv \sigma_i^x \sigma_{i+1}^x$, which corresponds on the lattice to the thermal primary field in the language of conformal field theory (CFT) [8,117].

On the other hand, quantum entanglement provides a powerful probe for quantum many-body systems. We partition the chain of length N into two equal parts $A = \{1, 2, \ldots, N/2\}$ and its complement. The half-chain entanglement entropy is defined as $S_{\mathrm{vN}} = -\mathrm{Tr}[\rho_A \ln \rho_A]$, where ρ_A is the reduced density matrix of the subsystem A by tracing out its complement. For 1D critical states, S_{vN} usually scales logarithmically with the system size [periodic boundary condition is assumed here]: $S_{\mathrm{vN}}(N) = (c_{\mathrm{eff}}/3) \ln N + S_0$, where c_{eff} is the effective central charge, which is a universal data for the criticality and S_0 a nonuniversal constant. To further reveal the topological features, we analyze the entanglement spectrum, defined as the set of the eigenvalues $\{\xi_n\}$ of the entanglement Hamiltonian $\mathcal{H}_A \equiv -\ln \rho_A$. As indicated by the Li-Haldane conjecture [32,137], the low-lying part of $\{\xi_n\}$ mimics the edge excitation spectrum of the physical Hamiltonian, serving as a fingerprint for topological edge degeneracies.

In the study of critical behaviors of the QP cluster Ising model, proper averaging over the modulation phases ϕ_1 and ϕ_2 is essential. In the strong QP-modulation regime, correlation functions may oscillate in sign across different realizations. To prevent destructive interference during averaging, we compute the average of the absolute values of the correlations. The average over different samples is denoted by $\bar{\cdot}$, and for simplicity, the absolute value symbols $|\cdot|$ are implicitly assumed for correlations and string operators in the reported averaged results of this Letter.

Quasi-periodic SPT phase—In this section, we demonstrate that, under strong QP modulation, the cluster SPT phase is driven into an unconventional SPT phase that exhibits area-law entanglement scaling despite a vanishing bulk energy gap—a feature unique to QP systems, as we establish below.

We focus on the phases by considering the representative point $\overline{J} = \bar{g} = 1/2, h_J = 1, h_g = 2$, located in the lower-left region of the phase diagram Fig. 1(c). Finite-size scaling of the bulk energy gap [Fig. 4(a)] and the half-chain entanglement entropy [Fig. 4(b)] reveals that this phase is gapless yet obeys an area-law entanglement scaling, in sharp contrast to the conventional gapped cluster SPT phase. At first glance, this behavior appears counterintuitive, as one-dimensional gapless systems with short-range interactions are generally expected to exhibit logarithmic entanglement scaling [138,139]. We note that the fourfold degeneracy and the subsequent eightfold plateau reflect the combinatorial filling of the paired zero-energy and lowest-excited single-particle entanglement modes (see Supplemental Material, Sec. IB [125] for more details). By further analyzing the SPT string order parameter [Fig. 4(c)] and the entanglement spectrum [Fig. 4(d)], we demonstrate the surprisingly stability of the SPT order with a gapless bulk, a regime we term the QP-SPT phase, which is unique to systems with QP modulations. Examining this stability is highly nontrivial and cannot be easily captured by standard field theoretic methods since there is no disorder to average over, in contrast to disordered systems [140–142]. Specifically, field-theoretical approaches for disordered systems [143]—including the supersymmetric approach [144] and the replica method with perturbative renormalization group and ϵ-expansion [140–142,145]—rely on ensemble averaging over random disorder or calculations for short-range correlated randomness. In contrast, at the length scales $r < q_i$ of interest, the quasiperiodic systems studied here are deterministic and aperiodic, with long-range correlations. Consequently, no direct field-theoretical method has been developed for such deterministic structures. This fundamental distinction explains why standard approaches for disordered systems are not directly applicable and motivates our combination of exact solutions with numerical simulations.

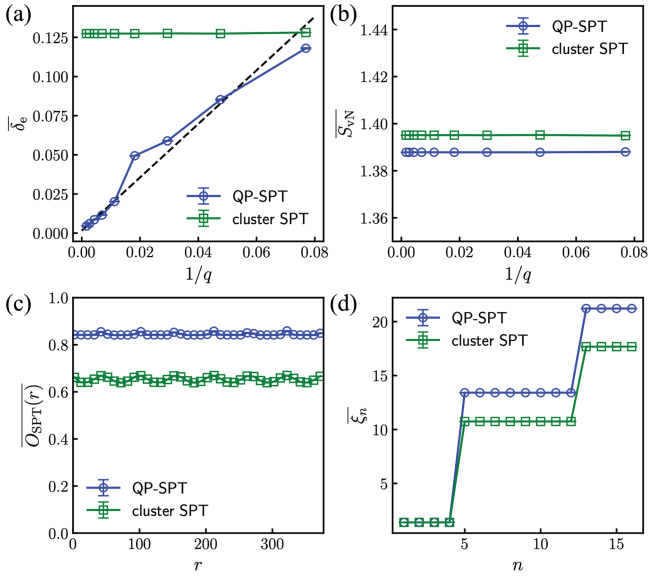


FIG. 4. (a) Energy gap $\overline{\delta_e}$ versus $1/q$ for QP-SPT and cluster SPT phases. The black dashed line represents a fit to the scaling form $\overline{\delta_e}(q) \sim A/q^{\omega} + \overline{\delta_e}(q \to \infty)$, yielding $\omega \approx 1.0(2)$ with $\overline{\delta_e}(q \to \infty) \approx 0.002(2)$. (b) Area-law scaling of the half-chain entanglement entropy $\overline{S_{vN}}$. (c) Scaling behavior of the SPT string order parameter $\overline{O_{SPT}(r)}$. (d) The bulk many-body entanglement spectrum $\overline{\xi_n}$. All results are obtained under PBC. Parameters: $\overline{J} = \bar{g} = 1/2, h_J = 1, h_g = 2$ [the left-pointing triangle in Fig. 1(c)] for QP-SPT and $\bar{J} = \bar{g} = 1/2, h_J = 1/2, h_g = 1/3$ [the right-pointing triangle in Fig. 1(c)] for cluster SPT. The parameter q ranges from 13 to 610 for (a), (b) and is fixed at $q = 377$ and 610, respectively, for (c) and (d).

To elucidate the underlying mechanism responsible for the emergence of the QP-SPT phase in QP systems, we note that the gapless nature of this regime originates from strong QP modulations that effectively fragment the chain, rendering the system an assembly of weakly connected, gapped cluster-spin subchains [see Fig. 1(b)]. Excitations localized near these weak links acquire arbitrarily low energies in the thermodynamic limit, i.e., $1/q \to 0$, leading to an overall gapless spectrum despite each individual subchain being gapped. Consequently, the gapless excitations are intrinsic to QP modulation and are not associated with rare-region effects, in sharp contrast to the Griffiths-McCoy phase in disordered spin chains [146–148]. By contrast, the entanglement structure and correlation properties are dominated by the universal behavior of each gapped subchain and are largely insensitive to the weak couplings. As a result, the system exhibits area-law entanglement scaling and long-range order in SPT string order parameters, analogous to conventional gapped SPT phases.

Comparison to the infinite-quasiperiodicity fixed point—It is noted that an infinite-quasiperiodicity fixed point has been found in Refs. [104,105] for Heisenberg and q-state Potts models. Crucially, the absence of an infinite-quasiperiodicity fixed point in our model is a distinct physical consequence of the Ising-like model, rather than a limitation of the strong-disorder renormalization group (SDRG) approach. In contrast to the Heisenberg or q-state Potts chains where strong quasiperiodic modulations preserve the quasiperiodic sequence structure under RG flows—leading to an infinite-quasiperiodicity fixed point with an activated dynamical scaling $\overline{\delta_e} \sim e^{-a \ln^2 L}$ and an infinite dynamical exponent $z = \infty$—the quasiperiodic sequence structure in the Ising case is not preserved. Consequently, the low-energy critical behavior remains governed by a quasiperiodic Ising fixed point featuring a finite dynamical exponent $z \approx 1.9$ and a power-law energy gap $\overline{\delta_e} \sim L^{-z}$ as reported in this Letter and previous literature [101,109].